Electronic Supplementary Information

From "Waste to Gold": One-pot Way to Synthesize Ultrafinely Dispersed Fe_2O_3-based Nanoparticles on N-doped Carbon for Synergistically and Efficiently Water Splitting

Diefeng Su[⊥], Jing wang[⊥], Haiyan Jin, Yutong Gong, Mingming Li, Zhenfeng Pang, Yong Wang*

Advanced Materials and Catalysis Group, ZJU-NHU United R&D Center, Department of Chemistry, Zhejiang University, Hangzhou 310028, P. R. China.

*Corresponding authors. Tel: (+86)-571-8827-3551, Fax: (+86)-571-8795-1895.
E-mail addresses: chemwy@zju.edu.cn.

[⊥] These authors contributed equally to this work.

Contents

Experimental

Materials

D-glucosamine hydrochloride (GAH), glucose, melamine and $Fe(NO_3)_3 \cdot 6H_2O$ were purchased from Aladdin. Nafion (5 wt.%) was purchased from Sigma-Aldrich. All the chemicals were used without further treatment.

Synthesis of Fe_2O_3/Fe@CN, Fe_2O_3/Fe@M, Fe_2O_3/Fe@G, Fe_2O_3/Fe@GL

The materials of Fe_2O_3/Fe@CN Fe_2O_3/Fe@M, Fe_2O_3/Fe@G and Fe_2O_3/Fe@GL were prepared with the same method except for different raw materials. Typically, a mixture solid of GAH (1g), melamine (20g) and $Fe(NO_3)_2 \cdot 6H_2O$ (1.67g) was ground into powder thoroughly, then directly calcined under a N_2 flow of 400 mL min^{-1}. The furnace was firstly heated to 600 ^oC and kept for 1h. Then the temperature was increased to 900 ^oC and held for 1h. Afterwards, the sample was cooled down to room temperature. Finally, the product was ground in the crucible and Fe_2O_3/Fe@CN was obtained. The materials of Fe_2O_3/Fe@M, Fe_2O_3/Fe@G and Fe_2O_3/Fe@GL were obtained from calcination of melamine with $Fe(NO_3)_2 \cdot 6H_2O$, GAH with $Fe(NO_3)_2 \cdot 6H_2O$, and glucose, melamine with $Fe(NO_3)_2 \cdot 6H_2O$, respectively.
Note: CN, G, M and GL represent nitrogen doped carbon, melamine, D-glucosamine hydrochloride (GAH) and glucose.

Synthesis of ph-Fe_2O_3/AC, Fe_2O_3/AC

ph-Fe_2O_3/AC was prepared by physically mixing Fe_2O_3 and AC and the ration of Fe_2O_3 and AC was under the same Fe content as Fe_2O_3/Fe@CN, which was defined according to ICP analysis. Fe_2O_3/AC was prepared with the same method according to previous report[1].

Characterization

SEM images were obtained from SU-70 microscope. Transmission electron microscopy (TEM) was carried out on HITACHI HT-7700 microscope at an acceleration voltage of 100 kV. High-resolution TEM (HRTEM), STEM-HAADF and STEM-EDX were performed on Tecnai G2 F30 S-Twin at an acceleration voltage of 300 KV. Powder X-ray diffraction (XRD) patterns were measured on a D/tex-Ultima TV wide angle X-ray diffractometer equipped with Cu Kα radiation (1.54 Å). The X-ray photoelectron spectra (XPS) were obtained with an ESCALAB MARK II spherical analyzer using an aluminum anode (Al 1486.6 eV) X-ray source. The Raman spectra were collected on a Raman spectrometer (JY, HR 800) using 514-nm laser. FT-IR spectra were recorded on a Nicolet Fourier transform infrared spectroscopy. N_2 adsorption analysis was performed at 77 K using a Micromeritics ASAP 2020 to investigate the surface areas and pore distributions. The specific surface area was calculated by Brunauere-Emmette-Teller (BET) method. The pore size distribution (PSD) plot was recorded by the BJH Desorption model. The Fe and N contents were measured by inductively coupled plasma (ICP) Analysis and Flash EA 1112 (Element Analysis), respectively.

Electrochemical measurements

HER Electrochemical measurements were conducted on a Gamry Reference 600 in an N_2 saturated 1 M KOH electrolyte at 25 ^oC with three-electrode setup. The Pt film and saturated calomel electrode were used as the counter electrode and reference electrode, respectively. All the electrochemical measurements in this paper were not corrected with IR-compensation. The working electrode was typically prepared as following: 3 mg catalyst was suspended in 500 μL ethanol with 50 μL Nafion solution to form homogeneous ink assisted by ultrasound. Then 10 μL of the ink was deposited onto the surface of glassy carbon by a micropipette and dried under room temperature. The final loading for all catalysts on work electrode is 0.28 mg cm^{-2}. The reversible hydrogen electrode (RHE) was defined as following:

|E (vs. RHE) |= | E (appl) + pH*0.059 + E (SCE) |, E (appl) referred as practical potential applied.

The potential range of linear sweep voltammetry was from 0.2 to -0.5 V (vs. RHE) and the scan rate was 5 mV s^{-1}. The estimation of the effective active surface area of the samples was obtained from cyclic voltammetry (CV) tests, which was performed at various scan rates (20, 40, 60 mV s^{-1}, etc.) in 0.1V − 0.2 V (vs. RHE). Tafel plots were tested under the potential from 0.2 to -0.5 V (vs. RHE) at the scan rate of 1 mV s^{-1}. Electrochemical impedance spectroscopy was performed at 0.25 V (vs. RHE). Time dependence of the current density was executed at 0.35 V (vs. RHE).

Figure S1. N1s XPS spectrum of Fe_2O_3/Fe@CN

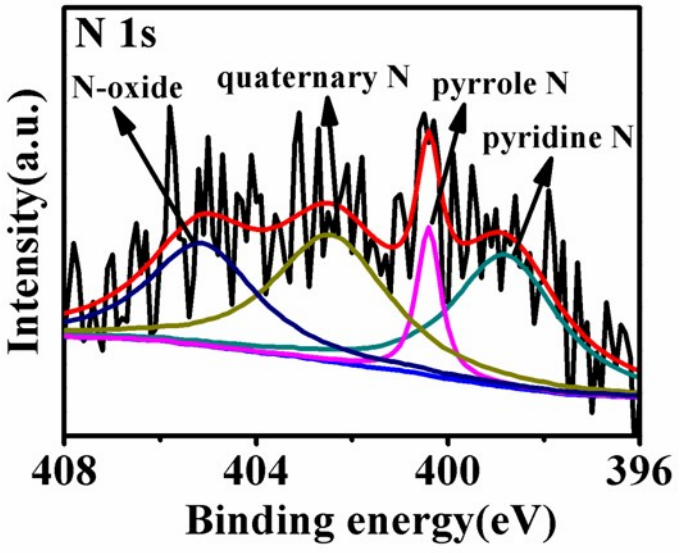

Figure S2. HRTEM image of Fe_2O_3/Fe@CN clearly showing the graphitic carbon

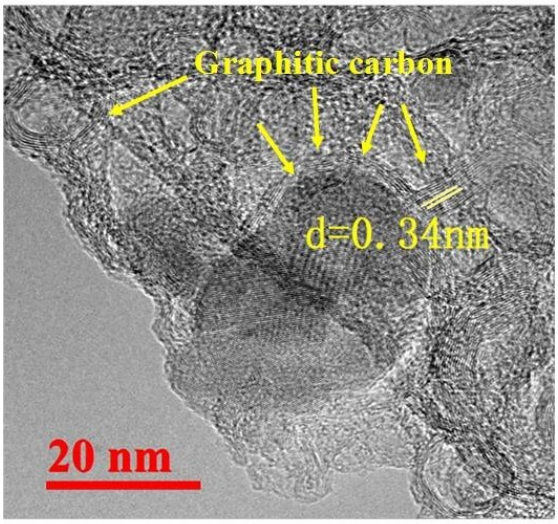

Figure S3. SEM images of Fe_2O_3/Fe@CN (a,b), Fe_2O_3/Fe@G (c), Fe_2O_3/Fe@M (d). Flake-like morphology and carbon nanotube was displayed in pictures (a, b), but aggregated particles were observed in pictures (c, d)

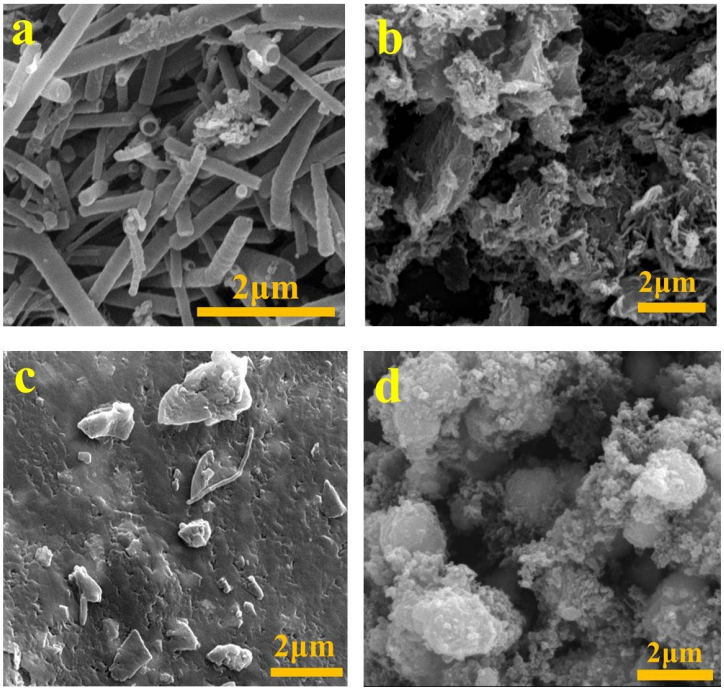

Figure S4. TEM images of Fe_2O_3/Fe@G (a), Fe_2O_3/Fe@M (b), Fe_2O_3/Fe@CN (c). It can be observed unarguable agglomeration appeared in (a,b). Nevertheless, well-dispersed NPs were shown in (c).

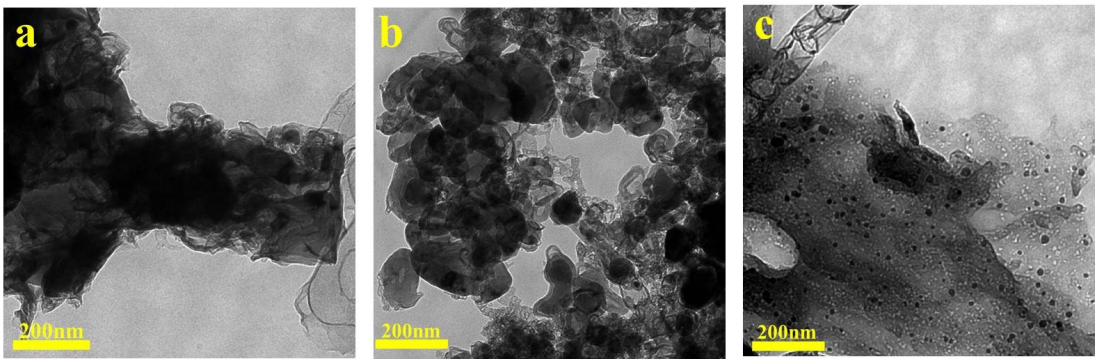

Figure S5. N content obtained via EA and semiquantitative analysis of XPS

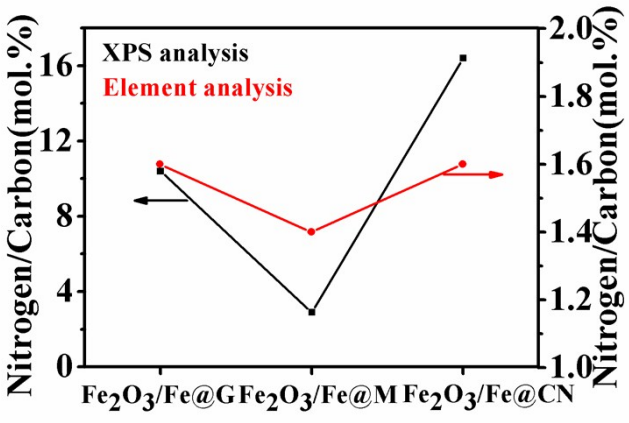

Figure S6. LSV of Fe_2O_3/Fe@CN with different loadings

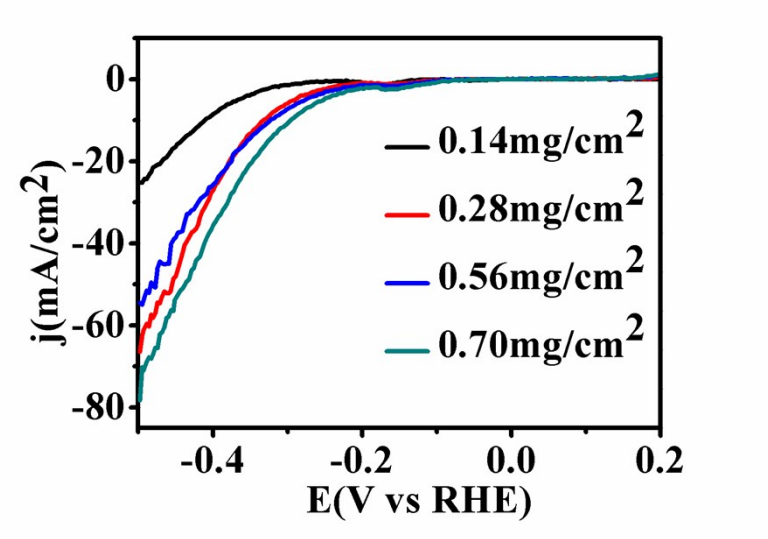

Figure S7. Optical photograph of the hybrid catalysts clearly illustrating H_2 bubble generated during LSV scan

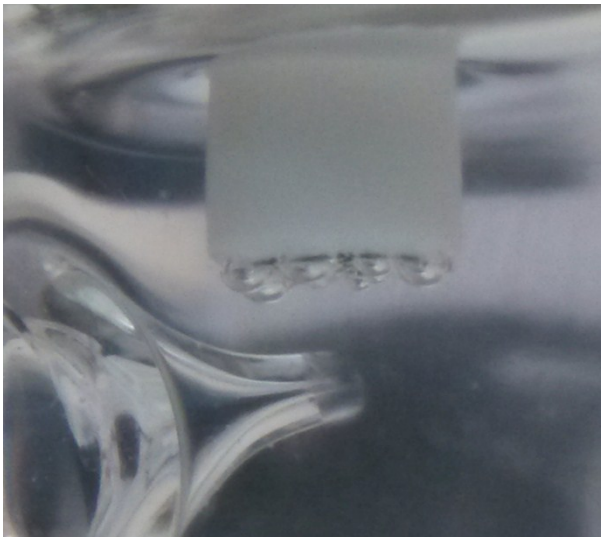

Figure S8. a), b) The TEM images of the as-prepared sample before and after electrochemical measurement respectively.

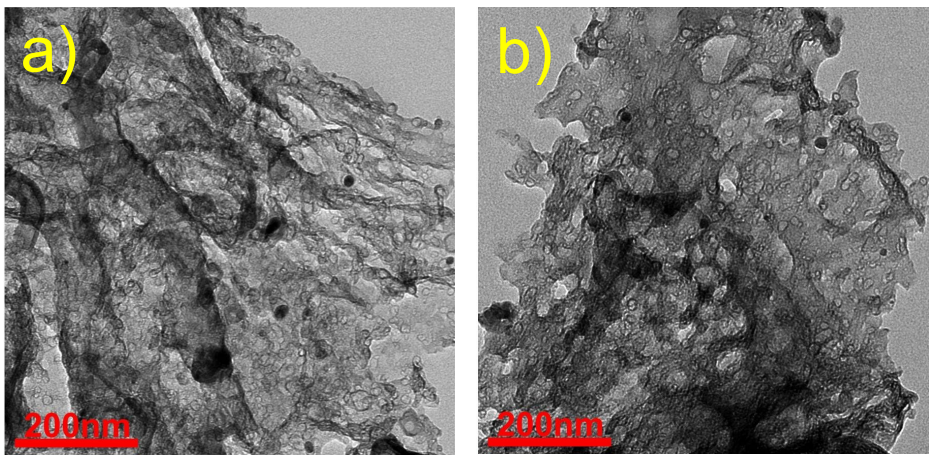

Note: the as-prepared sample was referred to the mixture of Fe_2O_3/Fe@CN and Nafion solution ready for the electrochemical measurement.

Figure S9. (a-c) Cyclic voltammetry curves of different samples at different scan rates under overpotential from 0.1 to 0.2 V (vs RHE). (d) The differences in current density variation (Δ J=Ja-Jc) at an overpotential of 0.15 V plotted against scan rate fitted to a linear regression enables the estimation of C_{dl}, where the slope is twice C_{dl}. Because the Cdl is proportional to the surface area and the conductivity of the materials, more effective active sites can be exposed for Fe_2O_3/Fe@CN, leading to the excellent HER activity

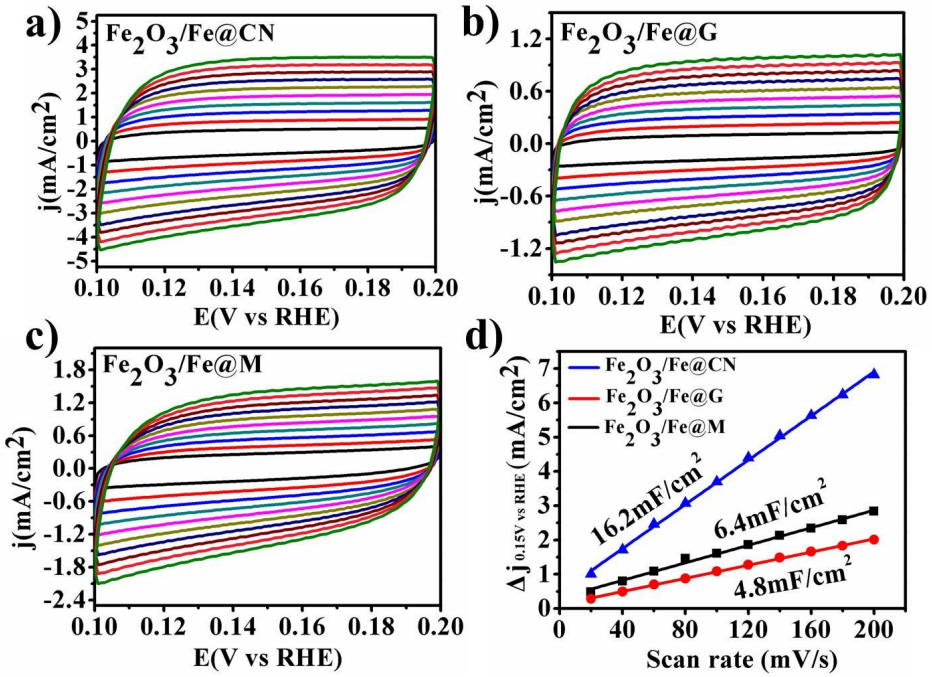

Figure S10. TEM image (a) and adsorption / desorption isotherms (a) of Fe_2O_3/Fe@GL, N/C content analysis (c) and LSV curve (d) of Fe_2O_3/Fe@GL & Fe_2O_3/Fe@CN

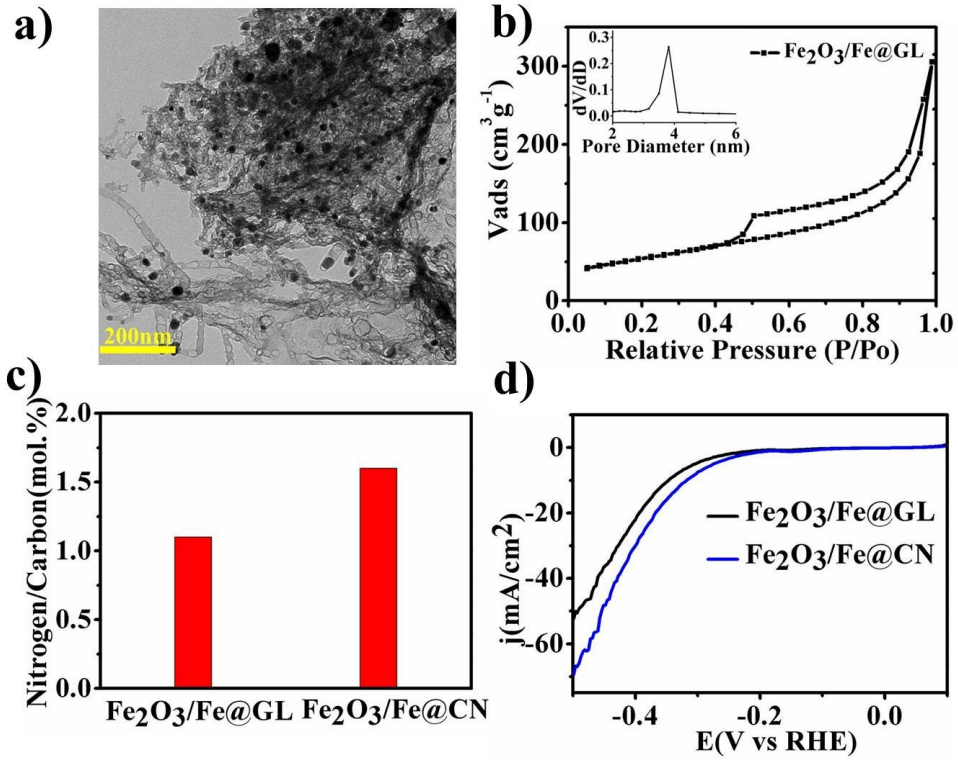

Figure S11. Raman spectra showing obvious raman-shift of Fe_2O_3/Fe@CN compared with Fe_2O_3

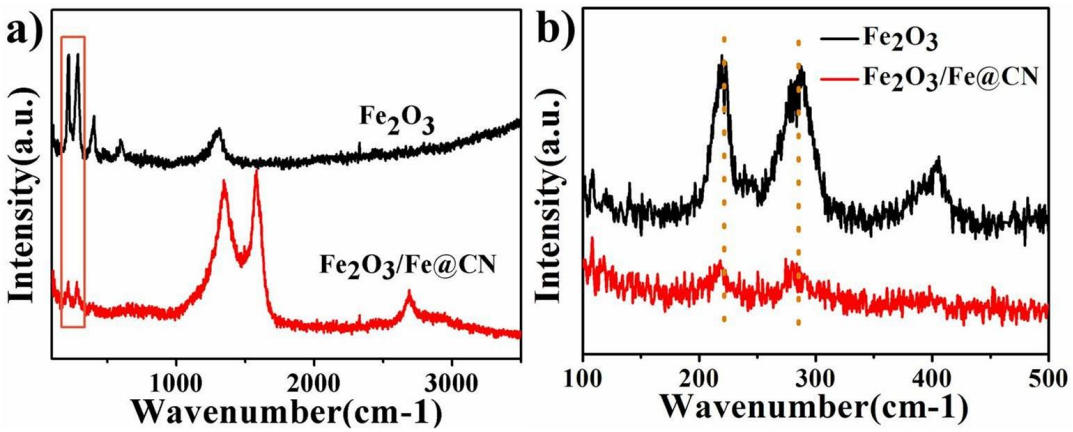

Figure S12. O1s XPS spectrum for Fe_2O_3/Fe@CN demonstrated the existence of Fe-O-C bonding.

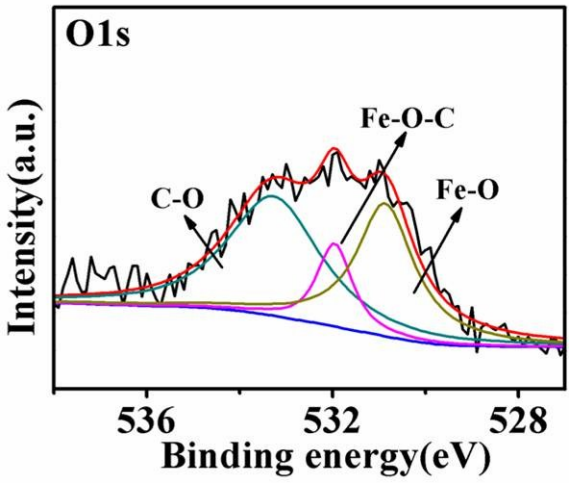

Figure S13. The HRTEM image of AT- Fe_2O_3/Fe@CN ,which was treated with 2M HNO_3 solution.

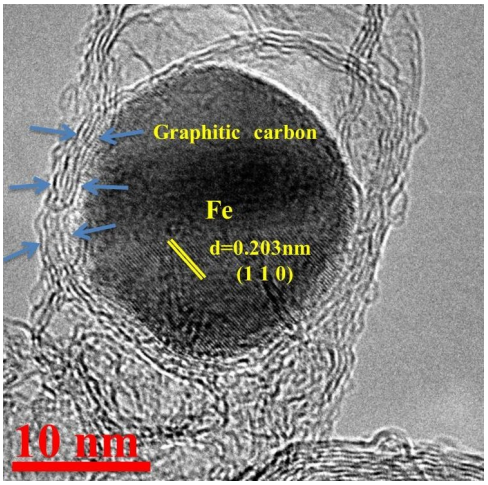

Figure S14. Fe 2p XPS spectrum for AT-Fe_2O_3/Fe@CN did not show the representative Fe signal.

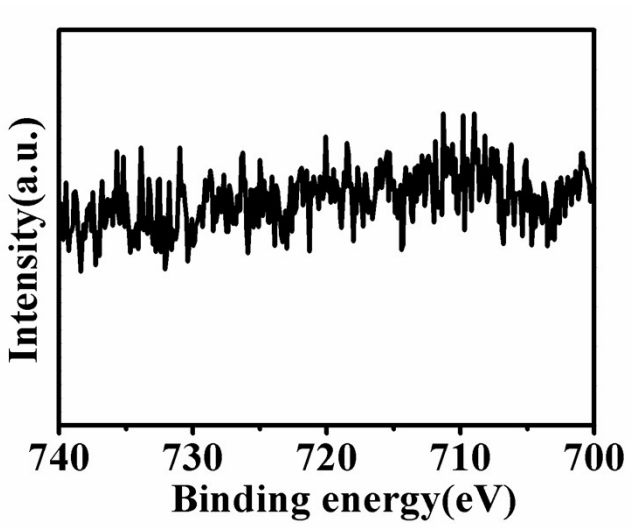

Figure S15. LSV of AT-Fe_2O_3/Fe@CN with different loadings

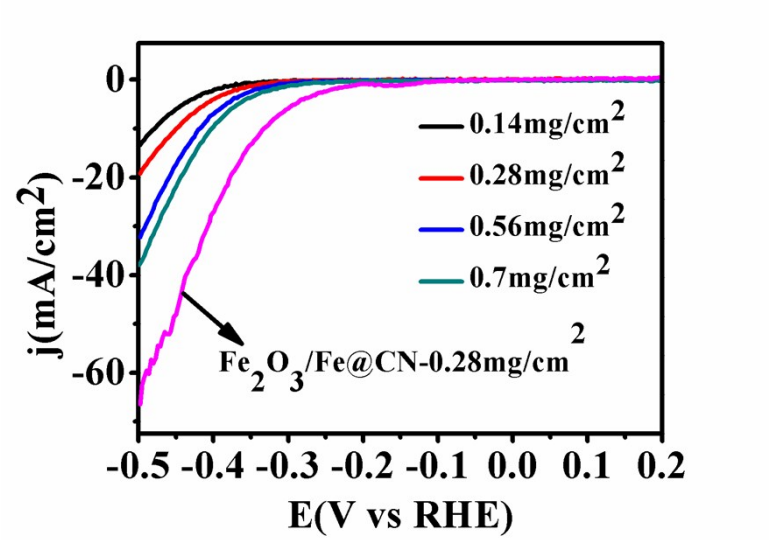

Figure S16. LSV (a), Tafel (b), XRD (c) and mole ratio of Fe to Fe_2O_3 (d) curves of catalysts made from different calcination temperature.

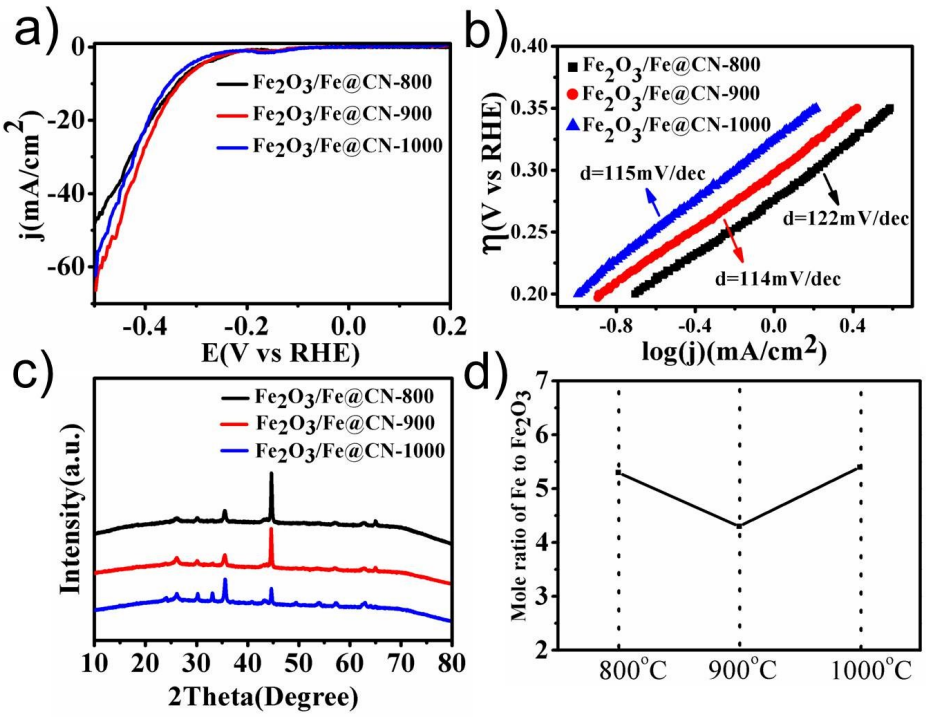

Table S1. N_2 sorption isotherms analysis of four different samples

	Specific Surface Area (m^2g^{-1})	Pore Size (nm)	Pore Volume (nm)
Fe_2O_3/Fe@M	**22**	**14.9**	**0.1**
Fe_2O_3/Fe@G	**88**	**5.0**	**0.1**
Fe_2O_3/Fe@CN	**233**	**7.8**	**0.6**
Fe_2O_3/Fe@GL	**193**	**8.2**	**0.5**
Fe_2O_3/Fe@CN-800	**168**	**9.0**	**0.5**
Fe_2O_3/Fe@CN-1000	**182**	**8.5**	**0.5**

Table S2. Comparison of the electrocatalytic activity of Fe_2O_3/Fe@CN via some representative solid-state HER catalysts recently reported

Catalyst	electrolyte	Current density j (mA/cm^2)	η at the corresponding j (mV)	Ref
Ni wire	**basic**	**10 mA/cm^2**	**350 mV**	***ACS. Catal.* 2013,3,166**
Ni	**basic**	**10 mA/cm^2**	**400 mV**	***Angew. Chem. Int. Ed.* 2012, *51*, 12703.**
Co-NRCNTs	**basic**	**10 mA/cm^2**	**370 mV**	***Angew. Chem. Int. Ed. 2014, 53, 4372***
Electrodeposited cobaltsulfide	**basic**	**1 mA/cm^2**	**480 mV**	***J. Am. Chem. Soc. 2013, 135, 17699***
Amorphous MoSx	**basic**	**10 mA/cm^2**	**540 mV**	***Chem. Sci. 2011, 2, 1262***
NiO/Ni-CNT	**basic**	**10 mA/cm^2**	**<100 mV**	***Nat. commun. 2014. 4695***
Fe_2O_3/Fe@CN	**basic**	**10 mA/cm^2**	**330 mV**	***This work***
FeP nanosheets	**acid**	**10 mA/cm^2**	**~240 mV**	***Chem. Commun. 2013, 49, 6656***
bulk Mo_2C	**acid**	**1 mA/cm^2**	**204 mV**	***Energy Environ.Sci.* 2013, *6*, 943**
MoN/C	**acid**	**2 mA/cm^2**	**290 mV**	***Angew. Chem. Int. Ed.* 2012, *51*, 6131**
MoO_3-MoS_2/FTO	**acid**	**10 mA/cm^2**	**310 mV**	***Nano Lett.* 2011, *11*, 4168**

Reference

1.Y. Li, C. Zhu, T. Lu, Z. Guo, D. Zhang, J. Ma and S. Zhu, *Carbon*, 2013, **52**, 565-573.